

PAPER

ISSDE: A Monte Carlo implicit simulation code based on Stratonovich SDE approach of Coulomb collision^{*}

To cite this article: Yifeng Zheng *et al* 2021 *Chinese Phys. B* **30** 095201

View the [article online](#) for updates and enhancements.

ISSDE: A Monte Carlo implicit simulation code based on Stratonovich SDE approach of Coulomb collision*

Yifeng Zheng(郑艺峰), Jianyuan Xiao(肖建元)[†], Yanpeng Wang(王彦鹏),
Jiangshan Zheng(郑江山), and Ge Zhuang(庄革)

School of Nuclear Science and Technology, University of Science and Technology of China, Hefei 230026, China

(Received 16 November 2020; revised manuscript received 15 March 2021; accepted manuscript online 18 March 2021)

A Monte Carlo implicit simulation program, Implicit Stratonovich Stochastic Differential Equations (ISSDE), is developed for solving stochastic differential equations (SDEs) that describe plasmas with Coulomb collision. The basic idea of the program is the stochastic equivalence between the Fokker–Planck equation and the Stratonovich SDEs. The splitting method is used to increase the numerical stability of the algorithm for dynamics of charged particles with Coulomb collision. The cases of Lorentzian plasma, Maxwellian plasma and arbitrary distribution function of background plasma have been considered. The adoption of the implicit midpoint method guarantees exactly the energy conservation for the diffusion term and thus improves the numerical stability compared with conventional Runge–Kutta methods. ISSDE is built with C++ and has standard interfaces and extensible modules. The slowing down processes of electron beams in unmagnetized plasma and relaxation process in magnetized plasma are studied using the ISSDE, which shows its correctness and reliability.

Keywords: Fokker–Planck equation, Stratonovich SDE, implicit, slowing down process

PACS: 52.20.Fs, 52.25.Xz, 52.40.Mj, 52.50.Gj

DOI: [10.1088/1674-1056/abefc7](https://doi.org/10.1088/1674-1056/abefc7)

1. Introduction

With the development of high-performance computing technology, large-scale numerical simulation becomes popular and important in research of plasma problems, especially when investigating nonlinear and multi-scale processes. Plasma is a complex physical system which is constituted with electromagnetic fields and various charged particles, and in many plasma problems such as beam heating [1–3] and slowing down of fusion alpha particles, [4,5] collisional effects are crucial. For collisional plasma systems, a commonly used model is described by the well-known Fokker–Planck equation. However, the Fokker–Planck (FP) equation is extremely difficult to solve, either analytically or via direct numerical calculations. The main difficulty is that the FP equation is a six-dimensional partial differential equation, which requires an enormous amount of computation to integrate, and algorithms are hard to be implemented. [6,7] Usually to simplify the FP equation, researchers utilize the guiding center approximation or dimension reduction in the continuum (grid-based) methods. [8–10] Compared with the continuum methods, particle-based methods may be preferable for some reasons. For example, particle Monte Carlo methods are simple, direct and converge at a rate independent of the number of dimensions. For particle-based hybrid methods, they are efficient, especially for partially thermalized systems. [7,11] So with the Monte Carlo method and the stochastic equivalence between

the stochastic differential equations (SDEs) and FP equations, we can use SDEs to investigate collisional plasma problems numerically. The stochastic differential equation theory plays an important role in many scientific fields, such as biology, chemistry, epidemiology, mechanics, microelectronics, and economics. In the past few decades, besides the field of mathematics, researchers in engineering and physics have paid more attention on numerical simulations based on SDEs. In physics research, the applications of SDE cover molecular dynamics, neurodynamics, celestial dynamics. [12–14] A significant part of SDE theory is the correlation between SDEs and FP equations. The most used SDEs are the Itô SDE and the Stratonovich SDE, and the corresponding numerical methods have also been developed. Besides Itô integration and Stratonovich integration, recently researchers developed an A-type integration which has more physical meanings and can give a natural correspondence between stochastic and deterministic dynamics. The A-type integration can also give a direct connection between trajectory dynamics and the Boltzmann–Gibbs distribution which can be used to make numerical computation less demanding. [15–18] Many studies about plasma collision have been carried out with the Monte Carlo method according to the theory of SDEs. For example, Takizuka and Abe [19] introduced a binary collision model by a Monte Carlo method for particle simulations and this model can describe a collision integral of the Landau form; Eriksson *et al.* [20,21] constructed

*Project supported by the National MCF Energy R&D Program of China (Grant No. 2018YFE0304100), the National Key Research and Development Program of China (Grant Nos. 2016YFA0400600, 2016YFA0400601, and 2016YFA0400602), and the National Natural Science Foundation of China (Grant Nos. NSFC-11805273 and NSFC-11905220).

[†]Corresponding author. E-mail: xiao jy@ustc.edu.cn

a Monte Carlo operator for the orbit-averaged Fokker–Planck equation to study collisions and wave-particle interaction to improve the effectiveness of the Monte Carlo method. Cadjan and Ivanov^[22] studied the absorption coefficient of a laser pulse incident into a dense plasma using the Langevin method with the Coulomb collision. Sherlock^[23] used a particle-fluid hybrid Coulomb collision Monte Carlo method to study the phenomenon of electron beam incident into the plasma. Rosin *et al.*^[7] conducted Monte Carlo simulations with the Itô SDE. Zhang and del-Castillo-Negrete^[24] calculated the kinetic dynamic of escape electrons with a backward Monte Carlo’s method. Stevens^[25] studied the energy changes during slowing down process. However, previous investigations can only be applied to Lorentzian and Maxwellian plasmas, which are inaccurate for cases with non-Maxwellian distributed plasmas. For example, in particle-in-cell (PIC) simulations, distribution functions are discretized using particles, which can be very different from Maxwellian distributions.

In the present work, the Stratonovich SDE for Lorentzian plasmas, Maxwellian plasmas are reviewed, and we have developed the Stratonovich SDE for arbitrary Klimontovich distribution function of background plasmas. We have also developed a Monte Carlo simulation program ISSDE, which is suitable for solving the SDE of Coulomb collisional plasmas. ISSDE is developed with the C++ language. The design of its architecture considers the standard IO, and each part of the program is modularized so that the program is easy to be expanded and is also convenient to join the structure-preserving algorithm module. ISSDE includes the following features: (1) The evolution of the distribution function of the FP equation is replaced by the evolution of the particles’ dynamic trajectories of the Stratonovich SDE so that we can describe the particle dynamics and show the random evolution trajectories of particles. (2) It can be proved theoretically that the ensemble average of results obtained by the ISSDE program and the FP equation are consistent. (3) The diffusion part of particle motion is solved by the implicit midpoint method, which guarantees the exactly energy conservation property for the diffusion term of the collision. (4) The ISSDE can also calculate the collision effect of arbitrary Klimontovich plasmas, which is more useful for calculating collisions in PIC schemes. Additionally, we simulate the relaxation process and slowing down process of charged particles injected into unmagnetized and magnetized plasma by ISSDE. We have also verified that the ensemble-averaged evolutionary behavior of the sampling points simulated by ISSDE is consistent with the evolution of the distribution function described by the corresponding FP equation. In addition, for different species of incident particles with different initial distribution function in Maxwellian plasmas, we can obtain the distribution function and ensemble average of velocity, energy, and temperature of the incident

particles, which are verified with theoretical results.

2. The Stratonovich SDE for Lorentzian plasmas and Maxwellian plasmas

The primary purpose of the ISSDE simulation program is to solve the Stratonovich SDE, which is based on the stochastic equivalence of FP equations and SDEs. According to different definitions of integrals of the random variable, SDEs have many representations. The Itô SDE and the Stratonovich SDE are the ones that have been most used.^[26] Although these two representations can be transformed from one to another,^[27] the corresponding integral form, which differs from the well-known Riemann’s, must be adopted in the solving process. Therefore, in the numerical solution process, attention needs to be paid on what kind of integration it adopts. It is more preferable to model physical problems as the Stratonovich SDE because the corresponding Stratonovich integral satisfies the same ordinary chain rule as the Riemann integral. In the following, we give a short introduction of the stochastic equivalence between the FP equation and the Itô SDE, the transformation from the Itô SDE to the Stratonovich SDE, and obtain the corresponding Stratonovich SDEs based on some FP equations. For more detail information, excellent papers such as Refs. [26–29] can be referred. Considering the FP equation of Coulomb collision with the Rosenbluth MacDonald Judd (RMJ) potential, it can then receive the equivalent Stratonovich SDE.^[30] We firstly present two commonly used cases as examples, which are the Lorentzian and Maxwellian plasmas. For the case of background plasma with arbitrary distribution function, a scheme based on Cholesky decomposition will be provided.

2.1. Stochastic equivalence of the FP equation and the Stratonovich SDE

The collision integral of the FP equation and the Itô SDE are

$$\left(\frac{\partial f_a}{\partial t}\right)_c = \frac{\partial}{\partial v_{ai}}[-P_i(\mathbf{v})f_a + \frac{1}{2}\frac{\partial}{\partial v_{ak}}(Q_{ik}(\mathbf{v})f_a)], \quad (1)$$

$$dv_{ai} = F_i(\mathbf{v})dt + D_{ik}(\mathbf{v})dW_k, \quad (2)$$

where $P_i(\mathbf{v})$ is the friction coefficient, Q_{ik} is the diffusion coefficient, and f_a is the distribution function of particles. The velocity of the incident particle is v_{ai} while \mathbf{v} is the relative velocity between the incident particle and background particle. Here $F_i(\mathbf{v})$ and $D_{ik}(\mathbf{v})$ are determined functions, and W_k is the Wiener process.^[31] The stochastic process is defined on the probability space $(\mathbb{R}^{\mathbb{T}}, \mathcal{B}^{\mathbb{T}}, P^W)$, where $\mathbb{T} = [0, t_{\max}]$ and P^W is the measure induced by the Wiener process. $\mathcal{B}^{\mathbb{T}}$ is the Borel σ -algebra.^[31] The solution of the FP equation is the evolution of distribution function of incident particles, while the solution of the Itô SDE is the trajectory of a single particle among these particles. The solution to the FP equation is

stochastically equivalent to the weak solution of the Itô SDE if $F(v)$, $D(v)$ and $P(v)$, $Q(v)$ satisfy the following relation^[20]

$$F(v) = P(v), \quad D(v) = Q^{1/2}(v), \quad (3)$$

where the second equation means $Q_{ik}(v) = D_{ij}(v)D_{jk}(v)$.

For a given FP equation, only the distribution function specifies. One still has the freedom to choose a probability space, a Wiener process, and a random variable with the desired initial distribution.^[31] As the coordinates and velocity of each particle in the particle ensemble at the initial time is determined, with one Wiener process, the coordinates and velocities of each particle are unique at each moment of the evolution. These are the strong solutions of the Itô SDE, and the distribution comprised these strong solutions is a weak solution of the Itô SDE. The Itô SDE is an equation describing the random trajectories particles in a system. We can obtain the evolution of particle distribution function through statistical methods. The Fokker–Planck equation is an equation describing the evolution of particle distribution function. It is an equation that can describe the probability evolution in a certain speed interval. For different initial random variables that obey the same distribution function, the strong solutions are different for each moment with same or different Wiener processes, while the distributions formed by these strong solutions are the same. When only the evolution of the distribution function is concerned, the solution of the FP equation is stochastically equivalent to the weak solution of the Itô SDE.^[31]

To let readers have a better understanding of SDEs and their representations, we briefly introduce related ready knowledge in this section of the article. For more information, Refs. [26,27,31] can be referred. There are several representations of SDEs. The two major forms are the Itô SDE and the Stratonovich SDE. The differences between these two representations are the different definitions of the random variable integrals. With the relationship of these two integrals and the appropriate choice of the coefficients, these two representations can be equivalent. The definitions of Itô integral and Stratonovich integral are given below, followed by the equivalent relation of the Itô SDE and the Stratonovich SDE. On an interval $T = [a, b]$ let there be given a real diffusive Markov process $W(t)$, and let there be given a function $f(t, W)$ continuous in t . If, for the sequence of partitions $a = t_1^{(\Delta)} \dots < t_{n-1}^{(\Delta)} < t_n^{(\Delta)} = b$ of the interval T , the maximum time step $\Delta = \max(t_{k+1} - t_k)$ converges to zero as $n \rightarrow \infty$, then Itô integral is defined as

$$\int_a^b f(t, W_t) dW_t = \lim_{\Delta \rightarrow 0} \sum_{k=1}^{n-1} f(t_{k+1}, W_{k+1})(W_{k+1} - W_k), \quad (4)$$

and the Stratonovich integral is defined as

$$\int_a^b f(t, W_t) \circ dW_t = \lim_{\Delta \rightarrow 0} \sum_{k=1}^{n-1} f(\xi_{k+1}, W(\xi_{k+1}))(W_{k+1} - W_k),$$

$$\xi_{k+1} = \frac{t_{k+1} + t_k}{2}, \quad (5)$$

where “ \circ ” is used to represent the Stratonovich integral. The solution of an arbitrary SDE

$$dX_t = \mu(X_t, t)dt + \sigma(X_t, t)dW_t \quad (6)$$

is

$$X_{t_1} = X_{t_0} + \int_{t_0}^{t_1} \mu(X_t, t)dt + \int_{t_0}^{t_1} \sigma(X_t, t)dW_t, \quad t_1 \geq t_0. \quad (7)$$

The SDE will be the Itô SDE if the integral in Eq. (7) is the Itô integral. The SDE will be the Stratonovich SDE if the integral in Eq. (7) is the Stratonovich integral. A Stratonovich integral can be presented as the sum of an the Itô integral with a drift term

$$\begin{aligned} & \int_a^b f(t, W_t) \circ dW_t \\ &= \int_a^b f(t, W_t) dW_t + \frac{1}{2} \int_a^b \frac{\partial f(t, W_t)}{\partial W_t} dt, \end{aligned} \quad (8)$$

if the function $f(t, W_t)$ satisfies the convergence condition^[26]

$$\int_a^b \mathbb{E}[f(t, W_t)]^2 dt < \infty, \quad \int_a^b \mathbb{E}[\frac{\partial f(t, W_t)}{\partial W_t}]^2 dt < \infty. \quad (9)$$

The left-hand side of Eq. (8) is the Stratonovich integral while the first term of the right-hand side is the Itô integral, and the second term is the Riemann integral. Thus, the same stochastic process which is described by Eq. (2) now can be presented by the Stratonovich SDE

$$\begin{aligned} dX_t &= (\mu(X_t, t) - \frac{1}{2} \frac{\partial \sigma(X_t, t)}{\partial X_t} \sigma(X_t, t))dt \\ &+ \sigma(X_t, t) \circ dW_t, \end{aligned} \quad (10)$$

i.e., Eq. (2) can be present in the form of the Stratonovich SDE^[22]

$$dv_{ai} = G_i(v)dt + D_{ik}(v) \circ dW_k, \quad (11)$$

where

$$G_i = F_i - \frac{1}{2} D_{jk} \frac{\partial D_{ik}}{\partial v_{aj}}, \quad (12)$$

and $Q = \|Q_{ik}\|$ and $D = \|D_{ik}\|$ are non-negative definite symmetry matrices.

2.2. The Stratonovich SDE for Lorentzian plasmas

In this subsection, we obtain the Stratonovich SDE for Lorentzian plasmas which is equivalent to the FP equation with the RMJ potential. The friction coefficient P and the diffusion coefficient Q of the FP equation under the RMJ potential can be referred to Refs. [21,30,32],

$$P = \Gamma_a \frac{\partial \mathcal{H}_a}{\partial v_a}, \quad (13)$$

$$Q = \Gamma_a \frac{\partial^2 \mathcal{G}_a}{\partial v_a \partial v_a}, \quad (14)$$

where $\mathcal{H}_a, \mathcal{G}_a$ are the RMJ potential functions,

$$\mathcal{H}_a = \sum_b \frac{m_a + m_b}{m_b} \int dv_b f_b(v_b) \frac{1}{v}, \quad (15)$$

$$\mathcal{G}_a = \sum_b \int dv_b v f_b(v_b), \quad (16)$$

$$\Gamma_a = \frac{z_a^2 z_b^2 e^4}{4\pi \epsilon_0^2 m_a^2} \ln \Lambda. \quad (17)$$

The value of fraction and diffusion parameters are dependent on the distribution function of background plasmas. An approximation can be used for a certain distribution function. For Lorentzian plasmas, the captain collision is electron-ion collision, and the background plasma can be treated as cold matter, which means that the thermal velocity is 0 m/s and the distribution function can be treated as $f_b(v_b) \propto \delta(v_b) \propto (v_b - v_{b0})$, where v_{b0} is the velocity of background plasma. Taking the distribution function into the RMJ potential function, we can reach

$$\mathcal{H}_a = \sum_b \frac{m_a + m_b}{m_b} \frac{1}{|v_a - v_{b0}|}, \quad (18)$$

$$\mathcal{G}_a = \sum_b |v_a - v_{b0}|. \quad (19)$$

The component forms of the two coefficients are

$$P_i = -\frac{z_a^2 z_b^2 \ln \Lambda}{4\pi n_b} \frac{n_b^2 e^4}{m_a^2 \epsilon_0^2} \frac{m_a}{m_r} \frac{v_i}{v^3} = -\Gamma_a n_b \frac{m_a}{m_r} \frac{v_i}{v^3}, \quad (20)$$

$$\begin{aligned} Q_{ik} &= \frac{z_a^2 z_b^2 \ln \Lambda}{4\pi n_b} \frac{n_b^2 e^4}{m_a^2 \epsilon_0^2} \frac{1}{v} \left[\delta_{ik} - \frac{v_i v_k}{v^2} \right] \\ &= \Gamma_a n_b \frac{v^2 \delta_{ik} - v_i v_k}{v^3}, \end{aligned} \quad (21)$$

where

$$m_r = \frac{m_a m_b}{m_a + m_b}, \quad (22)$$

m_a, m_b are mass of species a and b, respectively; m_r is the reduced mass of species a and b, and z_a, z_b are the charge number of species a and b. The number density of specie b is n_b , $\ln \Lambda$ is the Coulomb logarithm, and $v = |v_a - v_b|$ is the relative velocity of incident particles and the background plasma. By inserting Eqs. (20) and (21) into Eq. (3), we can obtain

$$G_i = -\frac{m_a}{m_b} \Gamma_a n_b \frac{v_i}{v^3}, \quad (23)$$

$$D_{ik} = \sqrt{\frac{\Gamma_a n_b}{v}} \left(\delta_{ik} - \frac{v_i v_k}{v^2} \right). \quad (24)$$

Substituting them into the Stratonovich SDE (11) yields

$$dv_{ai} = -\frac{m_a}{m_b} \Gamma_a n_b \frac{v_i}{v^3} dt + \sqrt{\frac{\Gamma_a n_b}{v}} \left(\delta_{ik} - \frac{v_i v_k}{v^2} \right) \circ dW_k, \quad (25)$$

i.e.,

$$dv_a = -\frac{m_a}{m_b} \Gamma_a n_b \frac{v}{v^3} dt - \Omega(v) v \times (v \times dW). \quad (26)$$

It can be extended to the cases with the external field as

$$dv_a = -\frac{m_a}{m_b} \Gamma_a n_b \frac{v}{v^3} - \Omega(v) v \times (v \times dW) + \frac{F_L dt}{m_a}, \quad (27)$$

where F_L is the Lorentzian force and $\Omega(v) = \sqrt{\frac{\Gamma_a n_b}{|v|^5}}$.

2.3. The Stratonovich SDE for Maxwellian plasmas

For a more general case, the probability density distribution function of background plasma is shifting Maxwellian, i.e.,

$$\begin{aligned} f_b(v) &= \frac{n_b}{(2\pi)^{3/2} v_{Tb}} \exp\left(-\frac{(v_b - \bar{v}_b)^2}{2v_{Tb}^2}\right), \\ v_{Tb} &= \sqrt{\frac{T_b}{m_b}}, \end{aligned} \quad (28)$$

where n_b is the density of background plasma, v_b is the velocity of background plasma, \bar{v} is the average velocity of background plasma and v_{Tb} is the thermal velocity of background plasma. Taking the distribution function into the RMJ potential function, we obtain

$$\mathcal{H}_a = \sum_b \frac{m_a + m_b}{m_b} \frac{1}{\tilde{v}_a} \Phi(\eta), \quad (29)$$

$$\mathcal{G}_a = \sum_b \sqrt{2} v_{Tb} \left\{ \eta [\Phi(\eta) - \Psi(\eta)] + \frac{1}{\eta} \Phi(\eta) \right\}, \quad (30)$$

where $\tilde{v}_a = |v_a - \bar{v}_b|$, $\eta = \frac{\tilde{v}_a}{\sqrt{2} v_{Tb}}$, Φ is the error function

$$\Phi(x) = \frac{2}{\sqrt{\pi}} \int_0^x e^{-y^2} dy, \quad (31)$$

$$\begin{aligned} \Psi(x) &= -\frac{1}{2} \frac{d(\Phi(x)/x)}{dx} \\ &= -\frac{1}{2} \frac{1}{x^2} \Phi(x) - \frac{1}{2x} \Phi'(x), \end{aligned} \quad (32)$$

$$\Phi'(x) = \frac{2}{\sqrt{\pi}} e^{-x^2}. \quad (33)$$

Inserting Eqs. (29) and (30) into Eqs. (13) and (14), after some calculations we have

$$P_i = -\frac{m_a + m_b}{m_b} \frac{1}{2v_{Tb}^2} \mathcal{N} \tilde{v}_a, \quad (34)$$

$$Q_{ik} = \mathcal{M} \delta_{ik} - (\mathcal{M} - \mathcal{N}) \frac{\tilde{v}_{ai} \tilde{v}_{ak}}{\tilde{v}_a^2}, \quad (35)$$

where

$$\mathcal{M} = \Gamma_a n_b \frac{1}{\sqrt{2} v_{Tb}} \frac{\Phi(\eta) - \Psi(\eta)}{\eta}, \quad (36)$$

$$\mathcal{N} = 2\Gamma_a n_b \frac{1}{\sqrt{2} v_{Tb}} \frac{\Psi(\eta)}{\eta}. \quad (37)$$

Inserting Eqs. (34) and (35) into Eq. (12), we can obtain

$$G_i = -\frac{m_a + m_b}{m_b} \frac{1}{2v_{Tb}^2} \mathcal{N} \tilde{v}_{ai}$$

$$\begin{aligned}
 & -\frac{1}{4} \frac{1}{\tilde{v}_a} [\mathcal{M}' \tilde{v}_{ai} + \frac{\tilde{v}_{ai} \tilde{v}_{ak}}{\tilde{v}_a^2} \tilde{v}_{ak} (\mathcal{N}' - \mathcal{M}')] \\
 & + [\mathcal{M} - (\mathcal{M}\mathcal{N})^{1/2}] \frac{\tilde{v}_{ai}}{\tilde{v}_a^2} \\
 & = -\frac{m_a + m_b}{m_b} \frac{1}{2v_{Tb}^2} \mathcal{N} \tilde{v}_{ai} \\
 & - \frac{1}{4} \frac{1}{\tilde{v}_a} \mathcal{N}' \tilde{v}_{ai} + [\mathcal{M} - (\mathcal{M}\mathcal{N})^{1/2}] \frac{\tilde{v}_{ai}}{\tilde{v}_a^2}, \quad (38)
 \end{aligned}$$

$$D_{ik} = \mathcal{M}^{1/2} \delta_{ik} - (\mathcal{M}^{1/2} - \mathcal{N}^{1/2}) \frac{\tilde{v}_{ai} \tilde{v}_{ak}}{\tilde{v}_a^2}, \quad (39)$$

where

$$\mathcal{N}' = \Gamma_a n_b \frac{1}{v_{Tb}^2} \frac{\Phi(\eta) - (2\eta^2 + 3)\Psi(\eta)}{\eta^2}. \quad (40)$$

Substituting it to the Stratonovich SDE (11) yields

$$\begin{aligned}
 dv_{ai} & = -\frac{m_a + m_b}{m_b} \frac{1}{2v_{Tb}^2} \mathcal{N} \tilde{v}_{ai} dt \\
 & - \frac{1}{4} \frac{1}{\tilde{v}_a} \mathcal{N}' \tilde{v}_{ai} dt + [\mathcal{M} - (\mathcal{M}\mathcal{N})^{1/2}] \frac{\tilde{v}_{ai}}{\tilde{v}_a^2} dt \\
 & + \mathcal{M}^{1/2} dW_k - (\mathcal{M}^{1/2} - \mathcal{N}^{1/2}) \frac{\tilde{v}_{ai} \tilde{v}_{ak} dW_k}{\tilde{v}_a^2}, \quad (41)
 \end{aligned}$$

i.e.,

$$\begin{aligned}
 d\mathbf{v} & = \left\{ -\frac{m_a + m_b}{m_b} \frac{1}{2v_{Tb}^2} \mathcal{N} - \frac{1}{4} \frac{1}{\tilde{v}_a} \mathcal{N}' \right. \\
 & \left. + [\mathcal{M} - (\mathcal{M}\mathcal{N})^{1/2}] \frac{1}{\tilde{v}_a^2} \right\} \tilde{\mathbf{v}}_a dt \\
 & + \mathcal{N}^{1/2} d\mathbf{W} - (\mathcal{M}^{1/2} - \mathcal{N}^{1/2}) \frac{\tilde{\mathbf{v}}_a \times (\tilde{\mathbf{v}}_a \times d\mathbf{W})}{\tilde{v}_a^2}. \quad (42)
 \end{aligned}$$

It can be extended to the cases with the external field as

$$\begin{aligned}
 d\mathbf{v} & = \left\{ -\frac{m_a + m_b}{m_b} \frac{1}{2v_{Tb}^2} \mathcal{N} - \frac{1}{4} \frac{1}{\tilde{v}_a} \mathcal{N}' \right. \\
 & \left. + [\mathcal{M} - (\mathcal{M}\mathcal{N})^{1/2}] \frac{1}{\tilde{v}_a^2} \right\} \tilde{\mathbf{v}}_a dt \\
 & + \mathcal{N}^{1/2} d\mathbf{W} - (\mathcal{M}^{1/2} - \mathcal{N}^{1/2}) \\
 & \times \frac{\tilde{\mathbf{v}}_a \times (\tilde{\mathbf{v}}_a \times d\mathbf{W})}{\tilde{v}_a^2} + \frac{\mathbf{F}_L dt}{m_a}. \quad (43)
 \end{aligned}$$

2.4. The Stratonovich SDE for an arbitrary distribution function of background plasmas

Besides the above two commonly used background particle distributions, usually we do not know the specific distribution of background particles. However, sometimes through statistical methods, we can calculate the integral of the distribution function. The PIC simulation is such a case, in which electrons and ions are discretized as marker-particles. Therefore, it is very meaningful to get the Stratonovich SDE corresponding to the background particles which obey arbitrary distribution function. In this subsection we will obtain the Stratonovich SDE for an arbitrary Klimontovich distribution

function of the background particles. It covers the background particle distribution function information in \mathcal{H}_a and \mathcal{G}_a , so as in \mathbf{P} and \mathbf{Q} .

For an arbitrary distribution function of background particles, assuming that the order of integration and differentiation can be reversed and we obtain

$$\begin{aligned}
 \mathbf{P} & = \Gamma_a \frac{\partial \mathcal{H}_a}{\partial \mathbf{v}_a} \\
 & = -\Gamma_a \sum_b \frac{m_a + m_b}{m_a} \int d\mathbf{v}_b f_b(\mathbf{v}_b) \frac{\mathbf{v}}{v^3}, \quad (44)
 \end{aligned}$$

$$\begin{aligned}
 \mathbf{Q} & = \Gamma_a \frac{\partial^2 \mathcal{G}_a}{\partial \mathbf{v}_a \partial \mathbf{v}_a} \\
 & = \Gamma_a \sum_b \int d\mathbf{v}_b f_b(\mathbf{v}_b) \frac{I}{v} - \Gamma_a \sum_b \int d\mathbf{v}_b f_b(\mathbf{v}_b) \frac{1}{v} \frac{\mathbf{v}\mathbf{v}}{v^2}, \quad (45)
 \end{aligned}$$

where $v = |\mathbf{v}_a - \mathbf{v}_b|$. Therefore, we have

$$Q_{ik} = \Gamma_a \sum_b \int d\mathbf{v}_b f_b(\mathbf{v}_b) \frac{1}{v} \delta_{ik} - \Gamma_a \sum_b \int d\mathbf{v}_b f_b(\mathbf{v}_b) \frac{1}{v} \frac{v_i v_k}{v^2}. \quad (46)$$

The SDE diffusion coefficient D_{ik} and the FP equation diffusion coefficient Q_{ik} meet Eq. (3). The decomposition of positive-semidefinite symmetric matrix \mathbf{Q} is always possible but, in general, not unique. We provide one scheme to solve the SDE diffusion coefficient D_{ik} according to Cholesky decomposition.^[22] For the third-order Hermitian positive definite matrix Q_{ik} , the expression is

$$\mathbf{Q} = \begin{bmatrix} Q_{11} & Q_{21} & Q_{31} \\ Q_{21} & Q_{22} & Q_{32} \\ Q_{31} & Q_{32} & Q_{33} \end{bmatrix}. \quad (47)$$

After Cholesky decomposition, the lower triangular matrix D_{ik} is obtained as follows:

$$D_{11} = \sqrt{Q_{11}}, \quad (48)$$

$$D_{21} = \frac{Q_{21}}{D_{11}}, \quad (49)$$

$$D_{31} = \frac{Q_{31}}{D_{11}}, \quad (50)$$

$$D_{22} = \sqrt{Q_{22} - D_{21}^2}, \quad (51)$$

$$D_{32} = \frac{Q_{32} - D_{21} D_{31}}{D_{22}}, \quad (52)$$

$$D_{33} = \sqrt{Q_{33} - D_{31}^2 - D_{32}^2}. \quad (53)$$

Thus, we obtain

$$\mathbf{D} = \begin{bmatrix} D_{11} & 0 & 0 \\ D_{21} & D_{22} & 0 \\ D_{31} & D_{32} & D_{33} \end{bmatrix}. \quad (54)$$

According to Eq. (12), the expression of \mathbf{G} can be obtained. Because the integral is solved for the diffusion coefficient \mathbf{Q} in the FP equation, the part containing the differential in \mathbf{G} can be expressed as the differential of \mathbf{Q} . After some calculations, we have

$$G_1 = F_1 - \frac{1}{2} D_{11} \frac{\partial D_{11}}{\partial v_{a1}} - \frac{1}{2} D_{21} \frac{\partial D_{11}}{\partial v_{a2}} - \frac{1}{2} D_{31} \frac{\partial D_{11}}{\partial v_{a3}}$$

$$\begin{aligned}
 &= F_1 - \frac{1}{4} \frac{\partial Q_{11}}{\partial v_{a1}} - \frac{1}{4} \frac{D_{21}}{D_{11}} \frac{\partial Q_{11}}{\partial v_{a2}} - \frac{1}{4} \frac{D_{31}}{D_{11}} \frac{\partial Q_{11}}{\partial v_{a3}}, \quad (55) \\
 G_2 &= F_2 - \frac{1}{2} D_{11} \frac{\partial D_{21}}{\partial v_{a1}} - \frac{1}{2} D_{21} \frac{\partial D_{21}}{\partial v_{a2}} - \frac{1}{2} D_{22} \frac{\partial D_{22}}{\partial v_{a2}} \\
 &\quad - \frac{1}{2} D_{31} \frac{\partial D_{21}}{\partial v_{a3}} - \frac{1}{2} D_{32} \frac{\partial D_{22}}{\partial v_{a3}} \\
 &= F_2 + \frac{1}{4} \frac{D_{21}}{D_{11}} \frac{\partial Q_{11}}{\partial v_{a1}} - \frac{1}{2} \frac{\partial Q_{21}}{\partial v_{a1}} - \frac{1}{4} \frac{\partial Q_{22}}{\partial v_{a2}} \\
 &\quad + \frac{1}{4} \frac{D_{21}(D_{22}D_{31} - D_{21}D_{32})}{D_{11}^2 D_{22}} \frac{\partial Q_{11}}{\partial v_{a3}} \\
 &\quad - \frac{1}{2} \frac{D_{22}D_{31} - D_{21}D_{32}}{D_{11}D_{22}} \frac{\partial Q_{21}}{\partial v_{a3}} - \frac{1}{4} \frac{D_{32}}{D_{22}} \frac{\partial Q_{22}}{\partial v_{a3}}, \quad (56) \\
 G_3 &= F_3 - \frac{1}{2} D_{11} \frac{\partial D_{31}}{\partial v_{a1}} - \frac{1}{2} D_{21} \frac{\partial D_{31}}{\partial v_{a2}} - \frac{1}{2} D_{22} \frac{\partial D_{32}}{\partial v_{a2}} \\
 &\quad - \frac{1}{2} D_{31} \frac{\partial D_{31}}{\partial v_{a3}} - \frac{1}{2} D_{32} \frac{\partial D_{32}}{\partial v_{a3}} - \frac{1}{2} D_{33} \frac{\partial D_{33}}{\partial v_{a3}} \\
 &= F_3 + \frac{1}{4} \frac{D_{31}}{D_{11}} \frac{\partial Q_{11}}{\partial v_{a1}} - \frac{1}{2} \frac{\partial Q_{31}}{\partial v_{a1}} \\
 &\quad + \frac{1}{4} \frac{D_{21}(D_{21}D_{32} - D_{22}D_{31})}{D_{11}^2 D_{22}} \frac{\partial Q_{11}}{\partial v_{a2}} \\
 &\quad + \frac{1}{2} \frac{D_{22}D_{31} - D_{21}D_{32}}{D_{11}D_{22}} \frac{\partial Q_{21}}{\partial v_{a2}} \\
 &\quad + \frac{1}{4} \frac{D_{32}}{D_{22}} \frac{\partial Q_{22}}{\partial v_{a2}} - \frac{1}{2} \frac{\partial Q_{32}}{\partial v_{a2}} - \frac{1}{4} \frac{\partial Q_{33}}{\partial v_{a3}}. \quad (57)
 \end{aligned}$$

The differential of Q with respect to velocity can be expressed as

$$\begin{aligned}
 \frac{\partial Q_{ik}}{\partial v_{aj}} &= \frac{\partial}{\partial v_{aj}} \left(\Gamma_a \sum_b \int d\mathbf{v}_b f_b(\mathbf{v}_b) \frac{1}{v} \delta_{ik} \right. \\
 &\quad \left. - \Gamma_a \sum_b \int d\mathbf{v}_b f_b(\mathbf{v}_b) \frac{1}{v} \frac{v_i v_k}{v^2} \right) \\
 &= \Gamma_a \sum_b \int d\mathbf{v}_b f_b(\mathbf{v}_b) \frac{v_j}{v^3} \delta_{ik} - \Gamma_a \sum_b \int d\mathbf{v}_b f_b(\mathbf{v}_b) \\
 &\quad \times \left[-\frac{3v_j}{v^5} v_i v_k + \frac{1}{v^3} \delta_{ij} v_k + \frac{1}{v^3} \delta_{jk} v_i \right]. \quad (58)
 \end{aligned}$$

Bringing the expression of G_i into Eq. (11) and using the numerical solution or statistical methods to process the integration, we can use the Stratonovich SDE to research the dynamic behavior of incident particles with Coulomb collisions when the background particles are arbitrary distribution functions. Considering the marker-particles setting in the PIC simulation, compared with the actual situation, the number of particles used in each grid is reduced, and the value of $\partial Q_{ik}/\partial v_{aj}$ corresponding to the SDE coefficient is larger than the actual one. Thus, a correction is necessary for PIC simulation. Assuming that each marker-particle represents N_m real particles, the values of mass and charge of marker-particle are N_m times as the values of a real particle. Discretise the distribution function of marker-particle using the Klimontovich representation

$$f_b(\mathbf{x}_b, \mathbf{v}_b, t) = \sum_{n=1}^N \mathcal{S}(\mathbf{x}_b - \mathbf{x}_{bn}) \delta(\mathbf{v}_b - \mathbf{v}_{bn}), \quad (59)$$

where N is the number of marker-particle, \mathcal{S} is the shape function.^[33] We obtain the values of P_i , Q_{ik} and $\partial Q_{ik}/\partial v_{aj}$ of marker-particle as

$$P_i = -\Gamma_{ma} \sum_b \frac{m_a + m_b}{m_a} \sum_n^N \mathcal{S}(\mathbf{x} - \mathbf{x}_{bn}) \frac{v_i}{v^3}, \quad (60)$$

$$\begin{aligned}
 Q_{ik} &= \Gamma_{ma} \sum_b \sum_n^N \mathcal{S}(\mathbf{x} - \mathbf{x}_{bn}) \frac{1}{v} \delta_{ik} \\
 &\quad - \Gamma_{ma} \sum_b \sum_n^N \mathcal{S}(\mathbf{x} - \mathbf{x}_{bn}) \frac{1}{v} \frac{v_i v_k}{v^2}. \quad (61)
 \end{aligned}$$

$$\begin{aligned}
 \frac{\partial Q_{ik}}{\partial v_{aj}} &= \Gamma_{ma} \sum_b \sum_n^N \mathcal{S}(\mathbf{x} - \mathbf{x}_{bn}) \frac{v_j}{v^3} \delta_{ik} \\
 &\quad - \Gamma_{ma} \sum_b \sum_n^N \mathcal{S}(\mathbf{x} - \mathbf{x}_{bn}) \\
 &\quad \times \left[-\frac{3v_j}{v^5} v_i v_k + \frac{1}{v^3} \delta_{ij} v_k + \frac{1}{v^3} \delta_{jk} v_i \right]. \quad (62)
 \end{aligned}$$

Here $\Gamma_{ma} = N_m^2 \Gamma_a$ is the collision coefficient for marker-particle. In this situation, the distribution function of real particle is

$$f_b(\mathbf{x}_b, \mathbf{v}_b, t) = \sum_{n=1}^N \mathcal{S}(\mathbf{x}_b - \mathbf{x}_{bn}) \delta(\mathbf{v}_b - \mathbf{v}_{bn}) N_m. \quad (63)$$

Thus, we can obtain P_{ri} , Q_{rik} and $\partial Q_{rik}/\partial v_{aj}$ for real particles in the PIC simulation process

$$P_{ri} = -N_m \Gamma_a \sum_b \frac{m_a + m_b}{m_a} \sum_n^N \mathcal{S}(\mathbf{x} - \mathbf{x}_{bn}) \frac{v_i}{v^3}, \quad (64)$$

$$\begin{aligned}
 Q_{rik} &= N_m \Gamma_a \sum_b \sum_n^N \mathcal{S}(\mathbf{x} - \mathbf{x}_{bn}) \frac{1}{v} \delta_{ik} \\
 &\quad \times -N_m \Gamma_a \sum_b \sum_n^N \mathcal{S}(\mathbf{x} - \mathbf{x}_{bn}) \frac{1}{v} \frac{v_i v_k}{v^2}. \quad (65)
 \end{aligned}$$

$$\begin{aligned}
 \frac{\partial Q_{rik}}{\partial v_{aj}} &= N_m \Gamma_a \sum_b \sum_n^N \mathcal{S}(\mathbf{x} - \mathbf{x}_{bn}) \frac{v_j}{v^3} \delta_{ik} \\
 &\quad - N_m \Gamma_a \sum_b \sum_n^N \mathcal{S}(\mathbf{x} - \mathbf{x}_{bn}) \\
 &\quad \times \left[-\frac{3v_j}{v^5} v_i v_k + \frac{1}{v^3} \delta_{ij} v_k + \frac{1}{v^3} \delta_{jk} v_i \right]. \quad (66)
 \end{aligned}$$

Therefore, the relationship of the coefficient between real particle and marker-particle is

$$\mathbf{F}_r = \frac{1}{N_m} \mathbf{F}, \quad (67)$$

$$\mathbf{G}_r = \frac{1}{N_m} \mathbf{G}. \quad (68)$$

By inserting Eqs. (60)–(62) to Eqs. (3) and (55)–(57), the expression of \mathbf{F} and \mathbf{G} for marker-particle can be gained. Then with Eqs. (67)–(68) and Eq. (11), we can obtain the expression of the Stratonovich SDE for the arbitrary distribution function of the background plasma in the PIC simulation.

3. The algorithm format and programming of ISSDE

Once we have obtained the Stratonovich SDE, according to requirement of the Euler–Maruyama method and the definition of the Stratonovich integral, the Stratonovich SDE can be discretized to construct the Monte Carlo simulation program ISSDE containing the Coulomb collision effect. For electron collision, due to $m_e \ll m_i$, the change of moment and energy of ion is very small. The Lorentzian plasma model can then be used in the case that the background ion can be treated as cold, which means the thermal velocity of background ion is 0m/s. For ion-ion or electron-electron collision, the background electron and ion cannot be treated as still, so Eq. (43) will be used to take the background temperature into consideration. For Lorentzian plasmas, Eqs. (26) and (27) are the Stratonovich SDE for general types of test particles and the background plasma. This case can be more simplified according to the condition

$$m_r = \frac{m_a m_b}{m_a + m_b} = \frac{m_e m_i}{m_e + m_i}, \quad m_e \ll m_i, \quad (69)$$

and hence

$$\frac{m_e}{m_r} \approx 1. \quad (70)$$

The coefficients are now

$$P_i = -\Gamma_a n_b \frac{v_i}{v^3}, \quad Q_{ik} = \Gamma_a n_b \frac{v^2 \delta_{ik} - v_i v_k}{v^3}, \quad (71)$$

and the coefficient of the Stratonovich SDE are now

$$G_i = 0, \quad D_{ik} = \sqrt{\frac{\Gamma_a n_b}{v}} \left(\delta_{ik} - \frac{v_i v_k}{v^2} \right). \quad (72)$$

Substituting Eq. (72) into the Stratonovich SDE (11), we have

$$d\mathbf{v}_a = -\Omega(v)\mathbf{v} \times (\mathbf{v} \times d\mathbf{W}), \quad (73)$$

for the case with an external field, we have

$$d\mathbf{v}_a = -\Omega(v)\mathbf{v} \times (\mathbf{v} \times d\mathbf{W}) + \frac{\mathbf{F}_L dt}{m_a}. \quad (74)$$

3.1. The discretization of the Stratonovich SDE

Consider the simplified Stratonovich SDE for Lorentzian plasmas that needs to be solved numerically,

$$\begin{cases} d\mathbf{v} = -\Omega(v)\mathbf{v} \times (\mathbf{v} \times d\mathbf{W}), \\ d\mathbf{x} = \mathbf{v} dt. \end{cases} \quad (75)$$

Discretizing them according to the requirement of the Euler–Maruyama method and the definition of the Stratonovich integral, we have

$$\begin{cases} \mathbf{v}^{n+1} = \mathbf{v}^n - \Omega\left(\frac{\mathbf{v}^{n+1} + \mathbf{v}^n}{2}\right) \frac{\mathbf{v}^{n+1} + \mathbf{v}^n}{2} \\ \quad \times \left[\frac{\mathbf{v}^{n+1} + \mathbf{v}^n}{2} \times (\mathbf{W}^{n+1} - \mathbf{W}^n) \right], \\ \mathbf{x}^{n+1} = \mathbf{x}^n + \frac{\mathbf{v}^{n+1} + \mathbf{v}^n}{2} dt, \end{cases} \quad (76)$$

where the superscript n indicate the time step. For the algorithm of implicit midpoint format, the geometric relationship of each vector is shown in Fig. 1. From the cross product relationship shown in Eq. (76), we can see

$$\left(\frac{\mathbf{v}^{n+1} - \mathbf{v}^n}{2} \right)^2 + \left(\frac{\mathbf{v}^{n+1} + \mathbf{v}^n}{2} \right)^2 = (\mathbf{v}^n)^2 = (\mathbf{v}^{n+1})^2. \quad (77)$$

Therefore, for a Lorentzian plasma, the implicit midpoint format is exactly energy conservative. As the equation is implicit, it can be iteratively solved by the Newton–Raphson method.^[34–36]

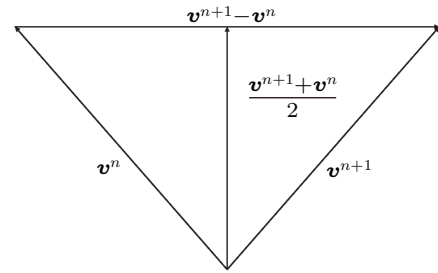


Fig. 1. The geometric relationship of each vector in the implicit midpoint format in the case of the Lorentzian plasma.

For the Stratonovich SDE of a Maxwellian plasma, the discrete process is similar, while the nonlinear equations are solved iteratively by the more stable Broyden method.^[37]

3.2. A splitting method for dynamics of charged particles with Coulomb collision

When there is a complex external field, using conventional algorithms to calculate the Stratonovich SDE may not have long-term stability because of the accumulation of numerical errors. In order to improve the stability of the numerical algorithm, a splitting method is used. The equations that ISSDE mainly requires to be solved are

$$\begin{cases} d\mathbf{x} = \mathbf{v} dt, \\ d\mathbf{v} = \frac{q}{m} \mathbf{E} dt + \frac{q}{m} \mathbf{v} \times \mathbf{B} dt + \mathbf{a}_c dt, \end{cases} \quad (78)$$

where \mathbf{a}_c is the acceleration caused by the Coulomb collision. For the Lorentzian plasma,

$$\mathbf{a}_{cL} dt = -\frac{m_a}{m_b} \Gamma_a n_b \frac{\mathbf{v}}{v^3} dt - \Omega(v)\mathbf{v} \times [\mathbf{v} \times d\mathbf{W}], \quad (79)$$

and for the Maxwellian plasma,

$$\begin{aligned} \mathbf{a}_{cM} dt = & \left[-\frac{m_a + m_b}{m_b} \frac{1}{2v_{Tb}^2} \mathcal{N} - \frac{1}{4} \frac{1}{\tilde{v}_a} \mathcal{N}' \right. \\ & \left. + [\mathcal{M} - (\mathcal{M}\mathcal{N})^{1/2}] \frac{1}{\tilde{v}_a^2} \right] \tilde{\mathbf{v}}_a dt \\ & + \mathcal{N}^{1/2} d\mathbf{W} - (\mathcal{M}^{1/2} - \mathcal{N}^{1/2}) \\ & \times \frac{\tilde{\mathbf{v}}_a \times (\tilde{\mathbf{v}}_a \times d\mathbf{W})}{\tilde{v}_a^2}. \end{aligned} \quad (80)$$

Equation (78) can be written as

$$\begin{cases} \frac{d\mathbf{x}}{dt} = \mathbf{v}, \\ \frac{d\mathbf{v}}{dt} = \frac{q}{m}\mathbf{E} + \frac{q}{m}\mathbf{v} \times \mathbf{B} + \mathbf{a}_c. \end{cases} \quad (81)$$

According to splitting method, the equation can be regarded as a vector field $\mathbf{F}(\mathbf{x}, \mathbf{v})$

$$\mathbf{F}(\mathbf{x}, \mathbf{v}) = \begin{bmatrix} \mathbf{v} \\ 0 \end{bmatrix} + \begin{bmatrix} 0 \\ \frac{q}{m}\mathbf{E} \end{bmatrix} + \begin{bmatrix} 0 \\ \frac{q}{m}\mathbf{v} \times \mathbf{B} \end{bmatrix} + \begin{bmatrix} 0 \\ \mathbf{a}_c \end{bmatrix}. \quad (82)$$

Therefore, the above system can be divided into four subsystems and then solved separately. These subsystems are

$$\phi_t^{F_1} : \begin{cases} \mathbf{x}(t) = \mathbf{x}_0 + t\mathbf{v}_0, \\ \mathbf{v}(t) = \mathbf{v}_0, \end{cases} \quad (83)$$

$$\phi_t^{F_2} : \begin{cases} \mathbf{x}(t) = \mathbf{x}_0, \\ \mathbf{v}(t) = \mathbf{v}_0 + tq\mathbf{E}(\mathbf{x}_0)/m, \end{cases} \quad (84)$$

$$\phi_t^{F_3} : \begin{cases} \mathbf{x}(t) = \mathbf{x}_0 + t\mathbf{v}_0, \\ \mathbf{v}(t) = \exp(-t\frac{q}{m}\hat{\mathbf{B}}(\mathbf{x}_0))\mathbf{v}_0, \end{cases} \quad (85)$$

where

$$\hat{\mathbf{B}}(\mathbf{x}) = \begin{bmatrix} 0 & -B_3(\mathbf{x}) & B_2(\mathbf{x}) \\ B_3(\mathbf{x}) & 0 & -B_1(\mathbf{x}) \\ -B_2(\mathbf{x}) & B_1(\mathbf{x}) & 0 \end{bmatrix}, \quad (86)$$

$$\phi_t^{F_4} : \begin{cases} \mathbf{x}(t) = \mathbf{x}_0, \\ \int d\mathbf{v} = \int \mathbf{a}_c dt. \end{cases} \quad (87)$$

The main purpose is that for the deterministic parts, which are $\phi_t^{F_1}$, $\phi_t^{F_2}$, $\phi_t^{F_3}$, we can use the volume-preserving algorithm to calculate, while the Coulomb collision part, which is $\phi_t^{F_4}$, still uses the Newton–Raphson method or the quasi-Newton method for calculation. In order to construct a second-order algorithm of implicit midpoint format similar to Boris algorithm, we can use such a combination

$$G_h^2 = \phi_{h/2}^{F_1} \circ \phi_{h/2}^{F_2} \circ \phi_{h/2}^{F_4} \circ \phi_h^{F_3} \circ \phi_{h/2}^{F_4} \circ \phi_{h/2}^{F_2} \circ \phi_{h/2}^{F_1}. \quad (88)$$

Then calculate each part separately. When there is no collision, it reduces to the normal Boris algorithm as^[38]

$$G_h^2 = \phi_{h/2}^{F_1} \circ \phi_{h/2}^{F_2} \circ \phi_h^{F_3} \circ \phi_{h/2}^{F_2} \circ \phi_{h/2}^{F_1}. \quad (89)$$

3.3. Design of the ISSDE simulation program

The ISSDE simulation program is implemented by the C++ programming language and can be used on Unix-like operating systems. It comprises I/O modules, initialization modules, particle pusher modules, parallel modules, field configuration modules, external force field modules, and other extensible modules. I/O modules call library functions from Lua^[39] and HDF5.^[40] The input files are Lua scripts so that users can

set parameters and physical problems conveniently and improve the efficiency of the program compilation. The output data is recorded and stored in the HDF5 format. It provides some static sampling methods in the initialization modules. The particle pusher module applies the algorithm given in Section 3.1 and other types of particle pusher functions, such as the collisionless volume-preserving algorithm and the Runge–Kutta algorithm. Parallel modules use the Message Passing Interface (MPI), these modules can sample the particles in parallel to speed up the calculation process. Field configuration and external force field configuration module include a variety of different configurations of the electromagnetic fields and external field, such as the radiation field and the gravity field. The extensible model is a script module that is written in Bash to enhance the scalability of the ISSDE simulation program.

3.4. ISSDE program flow chart

Figure 2 shows the flowchart of the ISSDE simulation program. The parallel program will be divided into multiple processes, each of which calculates the evolution of different particles in sequence. The I/O settings can be divided into Lua script as the input and configurations of the HDF5 file as the output. Lua script contains the basic parameters necessary for the program to run, including the basic physical parameters of the background plasma, the select switches of lots of configurations of the external fields, and the basic parameters of charged particles that need to be studied. The HDF5 file saves the coordinates and velocities of each particle in the phase space at each moment. The Wiener process and the corresponding coefficients contain the collision information of particles. We can get the value of W_t according to the definition of the Wiener process. The Wiener process is a stochastic process with the initial value $W_0 = 0$. The increment of W_t is a random variable that obeys a Gaussian distribution with dt as the variance and 0 as the mean value. According to the definition of the Wiener process, we can see that it is possible to generate values of the Wiener process for each moment once we know the number of steps that to be calculated and the time step of evolution. The value of W_t will then be brought into the quasi-Newton iteration loop of the main loop. Initial parameters will initialize the charged particle parameters, such as the particle’s initial position distribution, the initial velocity distribution, which is prepared for the main particle evolution loop. The main loop calculates the evolution of charged particles under the external field and the random force generated by the collision, and the data of each moment will be stored.

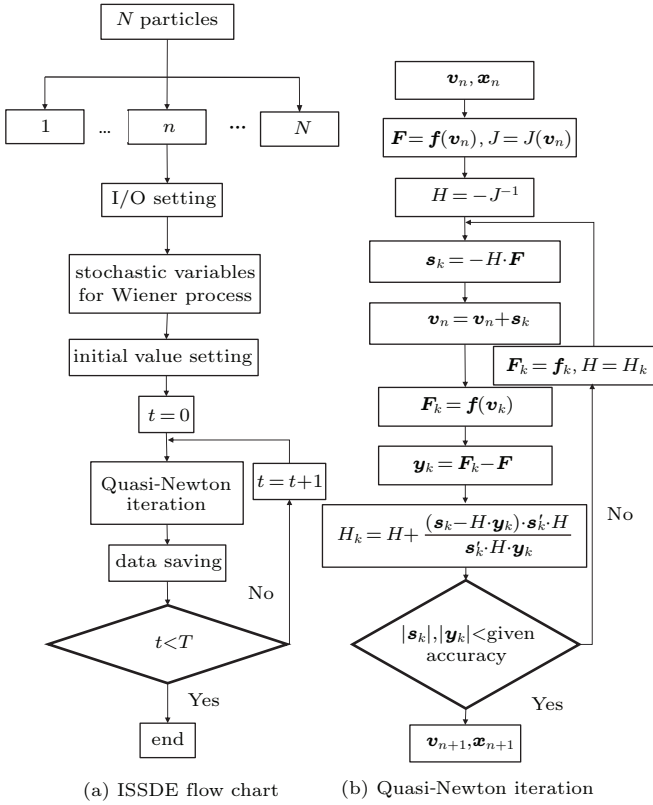


Fig. 2. Flow chart of the ISSDE and iteration of the quasi-Newton method.

4. Slowing down process in Lorentzian plasmas and Maxwellian plasmas

High-speed electron beam injection is a mechanism of unmagnetized plasma heating. The electron beam undergoes a slowing down process in the plasma and raises the local plasma temperature by transferring the kinetic energy to the plasma. Therefore, it is significant to study the effective mechanism of the slowing down process. In this section, slowing down processes are simulated using the ISSDE and compared with the results given by the solution of the FP equation. Not only the correctness of the ISSDE simulation can be verified, more physical information of the slowing down process can also be obtained through the Monte Carlo numerical simulation of the ISSDE.

4.1. Slowing down process of the electron beam in Lorentzian plasmas

In the calculation of particle slowing down process, we assume that the interactions between incident electrons and between background particles are negligible. Only scattering effects of background particles to incident particles are considered. Incident particles have the same velocity and their distribution function is

$$f_a(\mathbf{v}, t=0) = n_a \delta(\mathbf{v} - \mathbf{v}_0), \quad \mathbf{v}_0 = v_0 \mathbf{e}_1, \quad (90)$$

where the subscript a represents the incident particles, n_a is the number density of the incident particles, and v_0 is the velocity of the particles at $t=0$ with the initial direction \mathbf{e}_1 . The

general expression of the FP equation of the incident particles is

$$\begin{aligned} & \frac{\partial f_a}{\partial t} + \mathbf{v}_a \cdot \frac{\partial f_a}{\partial \mathbf{r}} + \frac{\mathbf{F}}{m_a} \cdot \frac{\partial f_a}{\partial \mathbf{v}_a} \\ & = \left(\frac{\delta f_a}{\delta t} \right)_c = - \frac{\partial}{\partial \mathbf{v}_a} \cdot \left(f_a \Gamma_a \frac{\partial \mathcal{H}_a}{\partial \mathbf{v}_a} \right) \\ & + \frac{1}{2} \frac{\partial^2}{\partial \mathbf{v}_a \partial \mathbf{v}_a} : \left(f_a \Gamma_a \frac{\partial^2 \mathcal{G}_a}{\partial \mathbf{v}_a \partial \mathbf{v}_a} \right). \end{aligned} \quad (91)$$

4.1.1. Theoretical approximation results of FP equation

Assuming that there is no external field in the background plasma, i.e. $\mathbf{E} = 0$ V/m, $\mathbf{B} = 0$ T, then $\mathbf{F}_L = 0$ N. Only the background plasma scattering effect of incident particles is taken into account. Therefore, the distribution function of the incident particles is the function of velocity and time, i.e., $f_a = f(\mathbf{v}, t)$, and we have $\frac{\partial f_a}{\partial \mathbf{r}} = 0$. Substituting it into the left-hand side of Eq. (91) yields

$$\left(\frac{\partial f_a}{\partial t} \right)_c = \frac{\partial f_a}{\partial t} + \mathbf{v}_a \cdot \frac{\partial f_a}{\partial \mathbf{x}} + \frac{\mathbf{F}_L}{m} \cdot \frac{\partial f_a}{\partial \mathbf{v}_a} = \frac{\partial f_a}{\partial t}, \quad (92)$$

and the FP equation of the incident particle is

$$\begin{aligned} \frac{\partial f_a}{\partial t} & = - \frac{\partial}{\partial \mathbf{v}_a} \cdot \left(f_a \Gamma_a \frac{\partial \mathcal{H}_a}{\partial \mathbf{v}_a} \right) \\ & + \frac{1}{2} \frac{\partial^2}{\partial \mathbf{v}_a \partial \mathbf{v}_a} : \left(f_a \Gamma_a \frac{\partial^2 \mathcal{G}_a}{\partial \mathbf{v}_a \partial \mathbf{v}_a} \right). \end{aligned} \quad (93)$$

Substituting the specific form of f_a into the equation and multiplying both sides with \mathbf{v}_a and then integrating it with respect to \mathbf{v}_b , we obtain

$$\begin{aligned} \frac{\partial}{\partial t} v_0 & = \Gamma_a \frac{\partial \mathcal{H}_a}{\partial v_a} \Big|_{v_a=v_0} \\ & = \Gamma_a \frac{m_a + m_b}{m_b} \frac{\partial}{\partial v_0} \int d\mathbf{v}_b f_b(v_b) \frac{1}{|v_0 - v_b|}. \end{aligned} \quad (94)$$

Let the background plasma obeys the following distribution

$$f_b(\mathbf{v}_b, t=0) = n_b \delta(\mathbf{v}_b - \mathbf{v}_{b0}), \quad (95)$$

where n_b and v_{b0} are the number density and bulk velocity of the background particle, respectively. Thus, the corresponding Rosenbluth potential is

$$\mathcal{H}_a(\mathbf{v}_b) = \frac{m_a + m_b}{m_b} \sum_b |v_a - v_{b0}|. \quad (96)$$

Substituting Eq. (95) into Eq. (94), we have

$$\frac{\partial v_0}{\partial t} = -n_b \Gamma_a \frac{m_a + m_b}{m_b} \frac{v_0 - v_{b0}}{|v_0 - v_{b0}|^3}. \quad (97)$$

We may define the slowing down time as

$$\tau_s(v_0) = - \frac{v_0}{\frac{\partial v_0}{\partial t}}, \quad (98)$$

and the corresponding slowing down frequency is

$$\nu_s(v_0) = n_b \Gamma_a \frac{m_a + m_b}{m_a} \frac{v_0 - v_{b0}}{v_0 |v_0 - v_{b0}|^3}. \quad (99)$$

This solution is consistent with the solution in Ref. [41].

4.1.2. Numerical results of the ISSDE in an unmagnetized Lorentzian plasma

Under the parameters shown in Table 1, we sample 10048 particles in total and make a statistical average of the entire incident particle system. The collision time between particles α and β is calculated by^[42]

$$\tau_{\alpha\beta} = \frac{3\sqrt{m_\alpha}T_\alpha^{3/2}\epsilon_0}{4\sqrt{2\pi}z_\alpha^2z_\beta^2\ln\Lambda e^4n_\beta}, \quad (100)$$

It shows the evolution of the averaged velocity of the incident particles parallel to the incident direction in Fig. 3. The result of the ISSDE program simulation shown by the dotted line and the result of the FP equation shown by the solid line described by Eq. (97) are in good agreement. The averaged velocity of incident particles parallel to the incident direction gradually decreases and then tends to be stable. The present result is consistent with Ref. [23], which used a different method to describe the slowing down process. This proves the correctness of using the ISSDE simulation program.

Table 1. The coefficients of the slowing down process without extra magnetic field, where τ_{ei} means the collision time between electrons and ions.

Variable	Parameter	Value
\boldsymbol{x}	Initial position (m)	(1.05, 0, 0)
\boldsymbol{v}	Initial velocity (m/s)	(5.5×10^6 , 0, 0)
Δt	Time step (s)	$1 \times 10^{-3} \tau_{ei}$
\boldsymbol{B}	Initial magnetic field strength (T)	(0, 0, 0)
n	Density of plasma (cm^{-3})	1.5×10^{14}
T_e	Temperature of electron in plasma (eV)	8
\boldsymbol{E}	Initial electric field strength (V/m)	(0, 0, 0)
T	Total number of time steps	80000

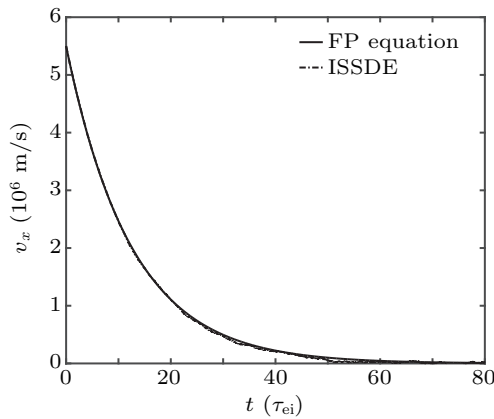


Fig. 3. The slowing down process of the electron beam along the incident direction (X-axis direction). The solid line represents the solution of the FP equation, while the dotted line represents the simulation result of the ISSDE.

4.1.3. Numerical results of the ISSDE in magnetized Lorentzian plasmas

For situations with external fields, the splitting method will be used and \boldsymbol{F}_L is added to the right-hand side of Eq. (75).

For the case of considering only the external uniform magnetic field, it can be seen from Eq. (74) that the incident particle system is in conservation of energy. Let the external magnetic field is along the z direction, and the magnetic field intensity is $B_0 = 2 \times 10^{-3}$ T. For electron-ion collision, the Lorentzian plasma model is used to simplify the calculation. The electron-ion collision can also be calculated by the Maxwellian plasma model, but the result is similar to that of the Lorentzian plasma. The evolution of the ensemble average of the energy of incident electrons in the Lorentzian and Maxwellian plasmas is calculated by the ISSDE. The result is shown in Fig. 4. The ensemble average of the energy is transferred in all directions because of the influence of the magnetic field and the Coulomb collision, and eventually all directions reach the same value, and the ensemble average of the total energy keeps unchanged.

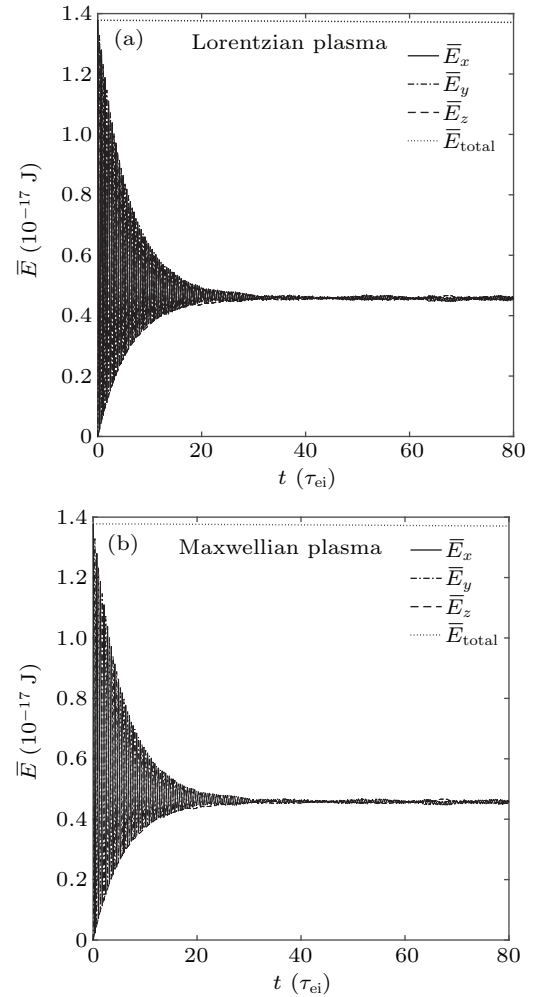


Fig. 4. The evolution of the ensemble-averaged energy of the incident electron beam in all directions in the magnetized plasma: (a) the background plasma is a Lorentzian plasma, (b) the background plasma is a Maxwellian plasma.

Taking advantage of the feature that the total energy is constant in a Lorentzian plasma, we use the two-stage stochastic Runge–Kutta method R2,^[43] the splitting method with two-stage stochastic Runge–Kutta method R2 in the collision part, and the splitting method with implicit point format in the collision part to calculate. Then we compared the relative error of

the ensemble-averaged energy. The result is shown in Fig. 5. It can be seen that when the time step is $5 \times 10^{-1} \tau_{ei}$, the numerical results obtained by the full stochastic Runge–Kutta method diverge, and the result of the split method is better than the result of the full stochastic Runge–Kutta method. The results of the splitting method with the implicit midpoint format in the collision part are better than the splitting method with the stochastic Runge–Kutta method. The relative error of the splitting method with the implicit midpoint format remains in the order of 10^{-10} when the error of the Newton–Raphson or the quasi-Newton method is 10^{-13} . Therefore, the splitting method with the implicit midpoint format in the collision part has certain advantages. For a one-dimensional one-Wiener process, stochastic Runge–Kutta methods such as CL, E1 and E2 have a convergence order of 1.5.^[44,45] However, for multi-dimensional multi-Wiener process, their convergence order will become 0.5. The implicit midpoint rule will not have such a problem, and the convergence order remains 1.0.

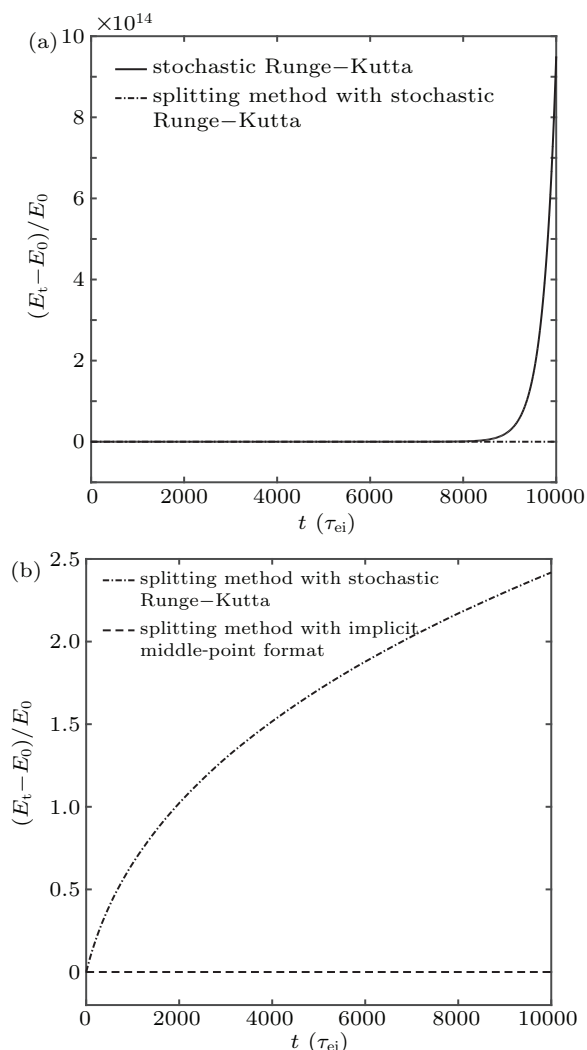


Fig. 5. The relative error of ensemble-averaged energy obtained by various methods. (a) The solid line is the result of the stochastic Runge–Kutta method, the dotted line is the result of the splitting method with stochastic Runge–Kutta method in the collision part. (b) The dashed line is the result of the splitting method with implicit midpoint format in the collision part.

4.2. Relaxation process of electrons with Maxwellian distribution in magnetized Maxwellian electrons

Compared with the Lorentzian plasma, the objective function and the derivative of the objective function in the Maxwellian plasma are much more complicated. The Jacobian matrix may be sparse or singular for the inappropriate choice of stochastic variables. Thus, for the Maxwellian plasma, we adopt a more stable Broyden method instead of the Newton–Raphson method to solve the nonlinear equations. As a benchmark, the incident particles are set as electrons with the same velocity distribution as the background magnetized Maxwellian electrons. The average velocity is 0 m/s and the temperature is 8 eV. Considering the relaxation process, if the incident electrons are constantly in thermal equilibrium and keep the temperature unchanged, the correctness of the program will be proven. As shown in Fig. 6, the temperature of the incident electron ensemble in all directions is mostly maintained around 8 eV. The consistency between the numerical results and the physical results shows the correctness of the ISSDE program.

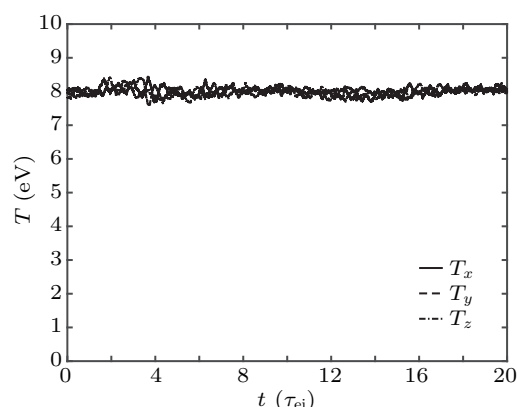


Fig. 6. Temperature evolution of electrons with Maxwellian distribution in magnetized Maxwellian electrons in three directions. Here τ_{ee} is the characteristic time of the electron–electron collision. The initial temperature of incident electrons is 8 eV as same as the background electrons.

4.3. Slowing down process of beams in the Maxwellian plasma

Neutral beam injection heating is one of the fundamental plasma heating methods. The injected high-energy neutral beam will turn into a high-energy ion beam through ionization and charge exchange with the background plasma. Then the high-energy ion beam will become thermal and deliver the energy to the background electrons and ions due to the collision, eventually reach thermal equilibrium with the background plasma. Using the ISSDE program, we can simulate the slowing down process of the incident particle beam. The evolution of the incident particle distribution function and the ensemble average of the physical quantities can then be calculated. In the following subsection, we simulate the slowing down process in the magnetized Maxwellian electrons when

the incident particles are electrons and ions. For electron-electron collision and ion-ion collision, the background electron and ion cannot be treated to be still, so the Eq. (43) will be used to take the background temperature into consideration.

4.3.1. Slowing down process of electron beams in magnetized Maxwellian electrons

For the case of magnetized plasma, the influence of an external field needs to be added to the equation. The parameters are set as follows: the external electric field intensity is $E = 0$ V/m, the external magnetic field is along the z direction, and the magnetic field intensity $B_0 = 2 \times 10^{-3}$ T. The direction of the electron beam is perpendicular to the direction of the magnetic field. The evolution of the ensemble-averaged velocity with time is shown in Fig. 7. Affected by the magnetic field, the momentum of the incident electrons continuously transfers around the directions that are perpendicular to the magnetic field. Due to the collision, the ensemble-averaged velocity gradually slows down, and finally drops to zero. This means that the ensemble-averaged kinetic energy of the particles is transformed due to the impact of the collision. The evolution of the ensemble average of the total energy in different directions is shown in Fig. 8.

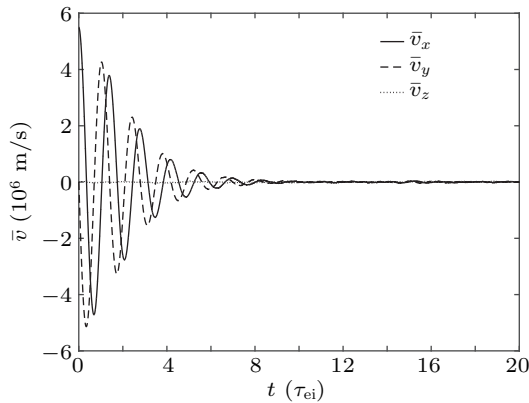


Fig. 7. Ensemble-averaged velocity evolution of electron beam in magnetized Maxwellian electron in three directions, with τ_{ee} being the characteristic time of the electron-electron collision.

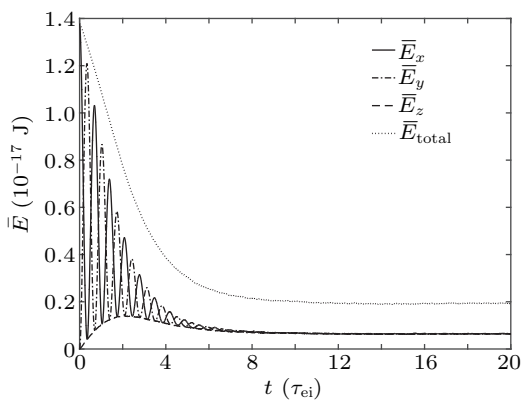


Fig. 8. Ensemble-averaged energy evolution of electron beam in magnetized Maxwellian electron in three directions. The dotted line indicates the evolution of ensemble-averaged total energy.

Because of the impact of collision, the ensemble average of the total energy decreases over time, and eventually keeps unchanged. The total energy of the electron beam is transferred to the background electrons by collision. The balance of the incident electron beam can be seen by the temperature evolution of the incident electron beam, as shown in Fig. 9. The total energy of the incident electrons is composed of the average kinetic energy and internal energy. During the slowing down process, part of the average kinetic energy transfers to the internal energy of the incident electrons, another part delivers to the background electrons. When the slowing down process is not violent, the average kinetic energy of the incident electrons will first transfer to the internal energy of the particles. Then the internal energy of the electrons will transfer to the background electrons in the form of heat conduction. Finally, the incident electrons and the background electrons reach thermal equilibrium. The evolution of the distribution function can reflect this more vividly, as shown in Fig. 10.

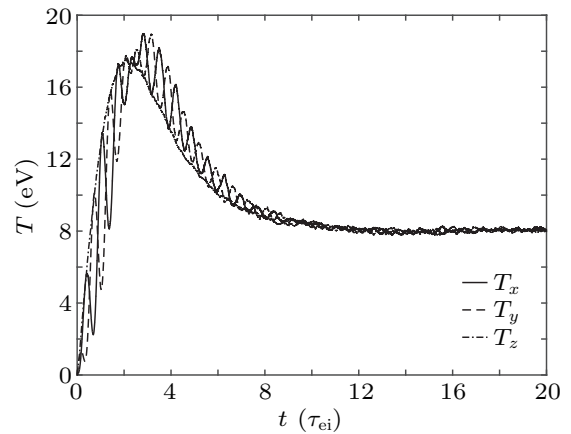


Fig. 9. Temperature evolution of electron beam in Maxwellian electron in three directions. The final equilibrium temperature in the three directions is 8 eV.

Under the influence of the magnetic field, the incident electrons rotate in the velocity space. The incident electrons go through the effects of slowing down and diffuse. The diffusion process is dominant at the beginning, so the distribution function gradually spreads in the velocity space. However, when the ensemble-averaged velocity of electrons constantly decreases, the slowing down process is dominant as the electron-electron collision cross-section becomes larger. As the slowing down process of the electrons becomes dominant, the distribution function of the incident particles tends to be a Maxwellian distribution function. When the particle temperature and the background reach equilibrium, the incident particle system has a Maxwellian distribution in the velocity space, and the corresponding standard deviation is the background electron temperature.

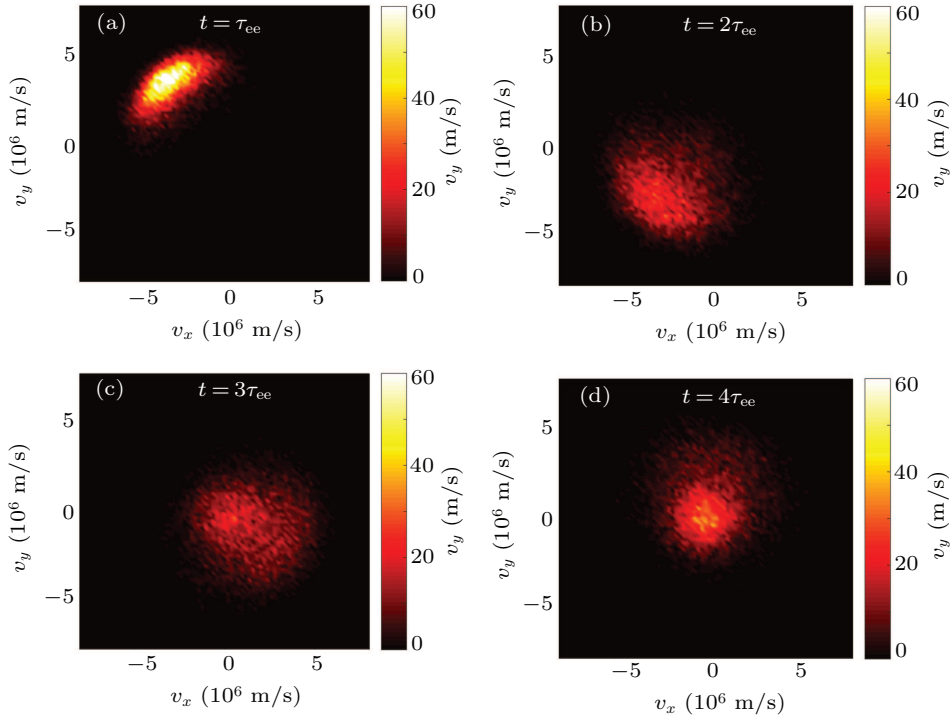


Fig. 10. Evolution of distribution function of incident electron beam in magnetized Maxwellian electrons in xy velocity space: (a) $t = \tau_{ee}$, (b) $t = 2\tau_{ee}$, (c) $t = 3\tau_{ee}$, (d) $t = 4\tau_{ee}$.

4.3.2. Slowing down process of ion beams in magnetized Maxwellian electrons

Consider an ion as a incident particle, and set the initial velocity of the incident ion to be 5.5×10^5 m/s, the evolution of the ensemble average of ion's velocity is shown in Fig. 9. When the relative velocity of the incident ion is small, the collision cross section between the ion and the electron will be large, so that the slowing down process is dominant. Compared with the ion cyclotron period, the time scale of ion-electron collision is about 250 times smaller. It can be seen that the ensemble-averaged velocity drops to zeros in about one or two ion cyclotron periods. The evolution of the ensemble average of the total energy of incident ions is shown in Fig. 12.

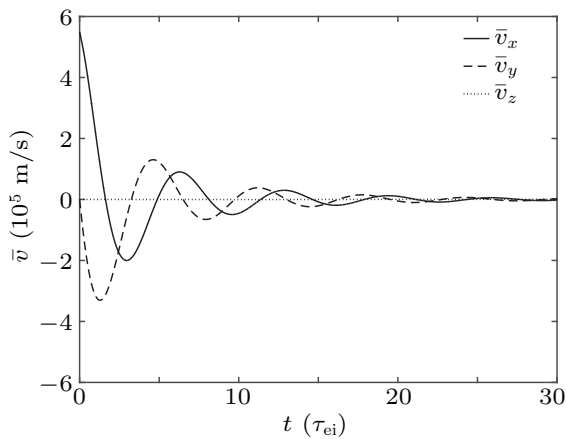


Fig. 11. Ensemble-averaged velocity evolution of ion beam in magnetized Maxwellian electron in three directions for initial velocity $v_x = 5.5 \times 10^5$ m/s, with τ_{ie} being the characteristic time of the ion-electron collision.

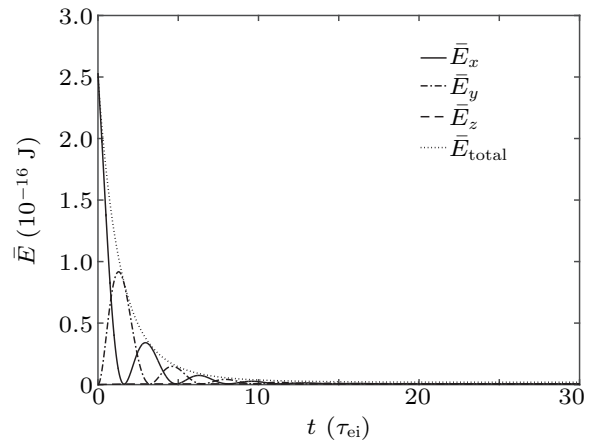


Fig. 12. Ensemble-averaged energy evolution of ion beam in magnetized Maxwellian electron in three directions. The dotted line indicates the evolution of ensemble-averaged total energy.

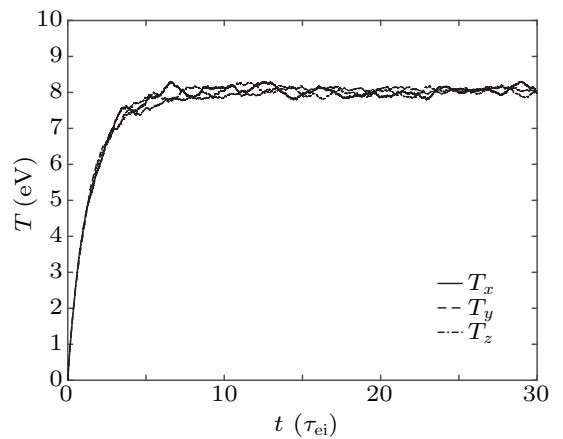


Fig. 13. Temperature evolution of ion beam in magnetized Maxwellian electron in three directions. The final equilibrium temperature in the three directions is very close to 8 eV.

Similar to the electron-electron collision, the total energy of the ion transfers to the background electron through the collision, and finally the incident ions and the background electrons reach equilibrium. Compared with electron-electron collisions, in the ion-electron collision process, the diffusion process of incident ions is not dominant compared to the slowing down process, this is because in the ion-electron collision process, most of the small-angle scattering occurs. The momentum exchange and energy exchange of ions and electrons in the ion-electron collision process are rapid when the slowing down process is dominant. This can be seen from the evolution of ensemble average of the incident ion temperature, as shown in Fig. 13. The rapid exchange of the momentum and

energy between the ion and electron makes most of the average kinetic energy of incident ions transfer to the background electrons and a small part of the average kinetic energy transfer to its own internal energy. The final ion temperature is consistent with the background electron temperature.

The evolution of the incident ion distribution function is shown in Fig. 14. The velocity in the x - y direction gradually drops to zero due to the slowing down process. The shape of the distribution function can reflect the diffusion process of collision. The diffusion process does not change as violent as the case of electron-electron collision because most of the small-angle scattering occurs.

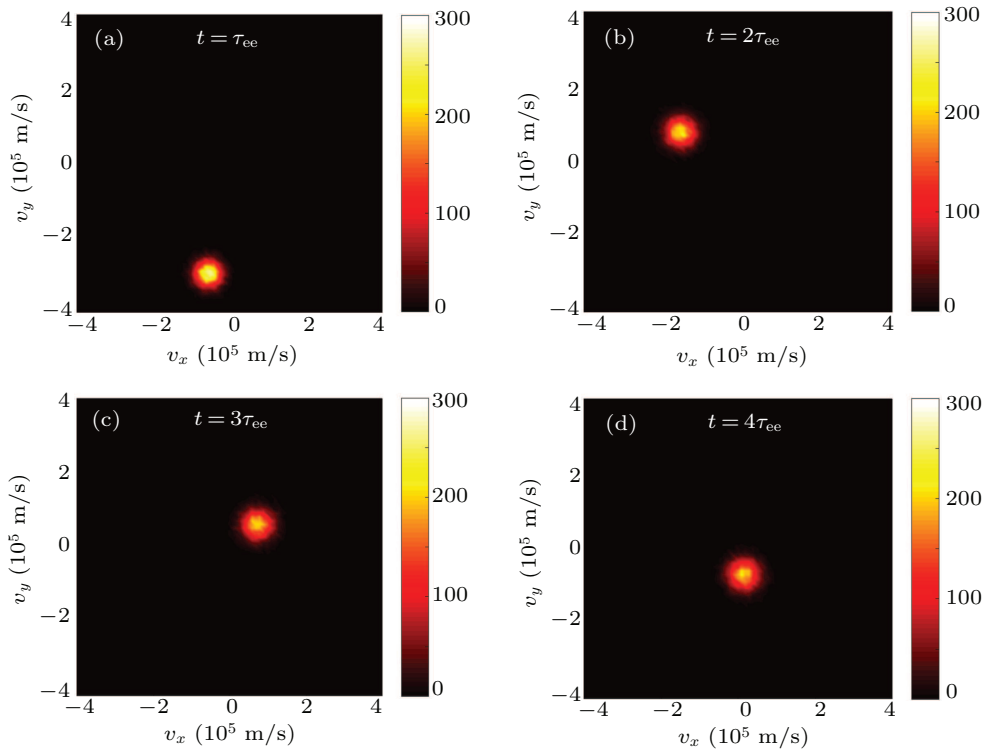


Fig. 14. Evolution of distribution function of ion beam in magnetized Maxwellian electron in xy velocity space: (a) $t = \tau_{ee}$, (b) $t = 2\tau_{ee}$, (c) $t = 3\tau_{ee}$, (d) $t = 4\tau_{ee}$.

5. Summary

Based on the stochastic equivalence between the Stratonovich SDE and the FP equation, the specific Stratonovich SDE equivalent to the FP equation with the RMJ potential is obtained. The splitting method and the implicit midpoint method are used to increase the numerical stability of the algorithm for dynamics of charged particles with Coulomb collision. The Monte Carlo implicit simulation program ISSDE for solving the Stratonovich SDE is developed to study the behavior of collisional plasma. Consider the background plasma as a Lorentzian plasma and a Maxwellian plasma. The ISSDE is used to simulate the slowing down process and relaxation process of different particles in the unmagnetized and magnetized plasmas. The consistency of the re-

sults obtained from the ISSDE simulation program with the results obtained from the FP equation about the slowing down process proves the accuracy of the ISSDE simulation program, and we can get more detailed physical information by the ISSDE.

The ISSDE simulation program can solve dynamic problems of the collisional plasma due to the simplicity of its implementation. When the distribution function of the incident particle ensemble becomes more complicated, the calculation with the FP equation becomes more difficult since the distribution function of the particle ensemble needs reconstruction in each calculation step. However, the ISSDE simulation program tracks the trajectories of individual particles directly. Therefore, once given the initial distribution of all particles in a charged particle system, all the information of the entire

charged particle ensemble at any time can be obtained.

As a Monte Carlo program, the present work ignores the influence of the self-consistent field on the particle ensemble. The consideration of self-consistent field is an important physical quantity that distinguishes the single-particle model from the kinetic model. The algorithm introduced in this article can be treated as a particle pusher module with Coulomb collision in the kinetic theory model such as SympPIC.^[38] The kinetic theory model describes the motion of charged particles under the effect of the self-consistent field and external field, which makes it more comprehensively to describe the behavior of plasma. However, most of the kinetic theory models are designed for collisionless plasma and it contains numerical collisions itself because of the choice of marker particle, discrete grid and shape of particles. It can significantly improve the research of advanced collisional algorithm if we apply the Stratonovich SDE to the traditional or some structure-preserving kinetic theory model and distinguish the real collision from the numerical collision clearly. We can consider the variational and canonical symplectic particle-in-cell (PIC),^[45–47] and the noncanonical symplectic PIC algorithm.^[38,48,49]

It is worth mentioning that according to the definition of kinetic integration which is a special limit of A-type integration,^[50–52] we can also obtain the kinetic SDE equivalent to FP equations. The kinetic integration can be defined in terms of Itô integration,^[53]

$$\int B(\mathbf{x}) \diamond d\mathbf{W} := \int B(\mathbf{x}) d\mathbf{W} + \frac{1}{2} \int \left[\frac{\partial}{\partial \mathbf{x}} \cdot D(\mathbf{x}) \right] dt, \quad (101)$$

where $D(\mathbf{x}) = B(\mathbf{x})B^T(\mathbf{x})$, “ \diamond ” is used to represent the kinetic integration. The kinetic SDE can then be obtained as follows:

$$\begin{aligned} dv_{ai} &= F_i(\mathbf{v})dt + D_{ik}(\mathbf{v})dW_k \\ &= K_i(\mathbf{v})dt + D_{ik}(\mathbf{v})\diamond dW_k, \end{aligned} \quad (102)$$

where

$$\begin{aligned} K_i &= F_i - \frac{1}{2} \frac{\partial}{\partial v_{aj}} Q_{ij} \\ &= F_i - \frac{1}{2} \frac{\partial D_{ik}}{\partial v_{aj}} D_{kj} - \frac{1}{2} D_{ik} \frac{\partial D_{kj}}{\partial v_{aj}}. \end{aligned} \quad (103)$$

For a Lorentzian plasma, we have

$$D_{ik} = \sqrt{\frac{\Gamma_a n_b}{v}} \left(\delta_{ik} - \frac{v_i v_k}{v^2} \right), \quad (104)$$

$$\begin{aligned} K_i &= F_i - \frac{1}{2} \frac{\partial D_{ik}}{\partial v_{aj}} D_{kj} - \frac{1}{2} D_{ik} \frac{\partial D_{kj}}{\partial v_{aj}} \\ &= -\frac{m_a}{m_b} \Gamma_a n_b \frac{v_i}{v^3}, \end{aligned} \quad (105)$$

Substituting K_i and D_{ik} into Eq. (102) we have

$$dv_{ai} = -\Gamma_a n_b \frac{m_a}{m_b} \frac{v_i}{v^3} dt + \sqrt{\frac{\Gamma_a n_b}{v}} \left(\delta_{ik} - \frac{v_i v_k}{v^2} \right) \diamond dW_k, \quad (106)$$

i.e.,

$$d\mathbf{v}_a = -\frac{m_a}{m_b} \Gamma_a n_b \frac{\mathbf{v}}{v^3} - \Omega(\mathbf{v})\mathbf{v} \times (\mathbf{v} \times d\mathbf{W}), \quad (107)$$

For a Maxwellian plasma, we have

$$\begin{aligned} K_i &= F_i - \frac{1}{2} \frac{\partial D_{ik}}{\partial v_{aj}} D_{kj} - \frac{1}{2} D_{ik} \frac{\partial D_{kj}}{\partial v_{aj}} \\ &= -\frac{m_a + m_b}{m_b} \frac{1}{2v_{Tb}^2} \mathcal{N} \tilde{v}_{ai} \\ &\quad - \frac{1}{2} \left[\frac{1}{2} \mathcal{N}' \frac{\tilde{v}_{ai}}{\tilde{v}_a} - 2[\mathcal{M} - (\mathcal{M}\mathcal{N})^{1/2}] \frac{\tilde{v}_{ai}}{\tilde{v}_a^2} \right] \\ &\quad - \frac{1}{4} \mathcal{N}' \frac{\tilde{v}_{ai}}{\tilde{v}_a} \\ &= -\frac{m_a + m_b}{m_b} \frac{1}{2v_{Tb}^2} \mathcal{N} \tilde{v}_{ai} - \frac{1}{2} \mathcal{N}' \frac{\tilde{v}_{ai}}{\tilde{v}_a} \\ &\quad + [\mathcal{M} - (\mathcal{M}\mathcal{N})^{1/2}] \frac{\tilde{v}_{ai}}{\tilde{v}_a^2}. \end{aligned} \quad (108)$$

Substituting Eq. (108) into Eq. (102), we have

$$\begin{aligned} dv_{ai} &= K_i dt + D_{ik} \diamond dW_k \\ &= -\frac{m_a + m_b}{m_b} \frac{1}{2v_{Tb}^2} \mathcal{N} \tilde{v}_{ai} dt \\ &\quad - \frac{1}{2} \mathcal{N}' \frac{\tilde{v}_{ai}}{\tilde{v}_a} dt + [\mathcal{M} - (\mathcal{M}\mathcal{N})^{1/2}] \frac{\tilde{v}_{ai}}{\tilde{v}_a^2} dt \\ &\quad + \mathcal{M}^{1/2} \diamond dW_i - (\mathcal{M}^{1/2} - \mathcal{N}^{1/2}) \frac{\tilde{v}_{ai} \tilde{v}_{ak}}{\tilde{v}_a^2} \diamond dW_k, \end{aligned} \quad (109)$$

i.e.,

$$\begin{aligned} d\mathbf{v} &= \left\{ -\frac{m_a + m_b}{m_b} \frac{1}{2v_{Tb}^2} \mathcal{N} - \frac{1}{2} \mathcal{N}' \frac{1}{\tilde{v}_a} \right. \\ &\quad \left. + [\mathcal{M} - (\mathcal{M}\mathcal{N})^{1/2}] \frac{1}{\tilde{v}_a^2} \right\} \tilde{\mathbf{v}}_a dt \\ &\quad + \mathcal{N}^{1/2} \diamond d\mathbf{W} - (\mathcal{M}^{1/2} - \mathcal{N}^{1/2}) \\ &\quad \times \frac{\tilde{\mathbf{v}}_a \times (\tilde{\mathbf{v}}_a \times d\mathbf{W})}{\tilde{v}_a^2}. \end{aligned} \quad (110)$$

Compared with the Stratonovich SDE, although the expression of kinetic SDE is not much different, we need to follow the definition of the kinetic integration to discrete it in numerical simulation. Hütter gave a definition of kinetic integration as^[53]

$$\begin{aligned} \int B(\mathbf{x}) \diamond d\mathbf{W} &:= ms - \lim_{M \rightarrow \infty} \sum_{i=1}^M \frac{1}{2} [D(\mathbf{x}_{i+1}) \cdot D_{inv}(\mathbf{x}_i) + 1] \\ &\quad \times B(\mathbf{x}_i) [\mathbf{W}_{i+1} - \mathbf{W}_i]. \end{aligned} \quad (111)$$

Moreover, the development of A-type integration equivalent to the Fokker–Planck equation with RMJ potential and the corresponding numerical methods can be good directions for research in plasma physics. In systems in which the drift term originates from a gradient of a potential that is mediated through the diffusion or mobility tensor, i.e.,

$$K(\mathbf{v}) = -\frac{1}{2} Q(\mathbf{v}) \left[\frac{\partial}{\partial \mathbf{v}} \phi(\mathbf{v}, t) \right], \quad (112)$$

the “Boltzmann–Gibbs distribution”

$$f(\mathbf{v}) \approx \exp[-\phi(\mathbf{v})] \quad (113)$$

is a stationary solution of Eq. (102). When we know expressions of $\mathbf{K}(\mathbf{v})$ and $Q(\mathbf{v})$, we may calculate $\phi(\mathbf{v})$ as

$$\phi(\mathbf{v}, t) = -2 \int Q^{-1}(\mathbf{v}) \mathbf{K}(\mathbf{v}) d\mathbf{v}. \quad (114)$$

It may not be very easy to calculate $\phi(\mathbf{v})$ as expressions of $\mathbf{K}(\mathbf{v})$ and $Q(\mathbf{v})$ are very complicated. The process of constructing the A-type SDE may be similar to that of the kinetic SDE. We will report related results elsewhere.

References

- [1] Janssen G C, Bonnie J, Granneman E, Kremontsov V and Hopman H 1984 *Phys. Fluids* **27** 726
- [2] Robertson S and Fisher A 1980 *J. Appl. Phys.* **51** 4094
- [3] Menon M M 1981 *Proc. IEEE Inst. Electr. Electron Eng.* **69** 1012
- [4] Ohnishi M and Ao N 1978 *Nucl. Fusion* **18** 859
- [5] Anderson D 1982 *Phys. Fluids* **25** 353
- [6] Thomas A G R, Tzoufras M, Robinson A P L, Kingham R J, Ridgers C P, Sherlock M and Bell A R 2012 *J. Comput. Phys.* **231** 1051
- [7] Rosin M S, Ricketson L F, Dimits A M, Cafilisch R E and Cohen B I 2014 *J. Comput. Phys.* **274** 140
- [8] Kerbel G and McCoy M 1985 *Phys. Fluids* **28** 3629
- [9] Epperlein E, Rickard G and Bell A 1988 *Comput. Phys. Commun.* **52** 7
- [10] Morel J 1981 *Nucl. Sci. Eng.* **79** 340
- [11] Ricketson L, Rosin M, Cafilisch R and Dimits 2014 *J. Comput. Phys.* **273** 77
- [12] Bossy M, Champagnat N, Maire S and Talay D 2010 *ESAIM-Math. Model. Numer. Anal.-Model. Math. Anal. Numer.* **44** 997
- [13] Capocelli R M 1971 *Kybernetik* **8** 214
- [14] Markov Y G and Sinitin I N 2004 *Cosmic. Res.* **42** 72
- [15] Yin L and Ao P 2006 *J. Phys. A: Math. Gen.* **39** 8593
- [16] Ao P, Kwon C and Qian H 2007 *Complexity* **12** 19
- [17] Shi J, Chen T, Yuan R, Yuan B and Ao P 2012 *J. Stat. Phys.* **148** 579
- [18] Yuan R and Ao P 2012 *J. Stat. Mech.* **2012** P07010
- [19] Takizuka T and Abe H 1977 *J. Comput. Phys.* **25** 205
- [20] Eriksson L G 1994 *Phys. Plasmas* **1** 308
- [21] Eriksson L G, Mantsinen M J, Hellsten T and Carlsson J 1999 *Phys. Plasmas* **6** 513
- [22] Cadjan M G and Ivanov M F 1999 *J. Plasma Phys.* **61** 89
- [23] Sherlock M 2008 *J. Comput. Phys.* **227** 2286
- [24] Zhang G N and Del-Castillo-Negrete D 2017 *Phys. Plasmas* **24** 092511
- [25] Stevens D E 2016 *Technical Report: A New Approach to Charged Particle Slowing Down and Dispersion* (U.S. Department of Energy Office of Scientific and Technical Information)
- [26] Kloeden P E and Platen E 2010 *Numerical Solution of Stochastic Differential Equations* (Springer Science & Business Media) p. 99
- [27] Stratonovich R L 1966 *SIAM J. Control* **4** 362
- [28] Kupferman R, Pavliotis G A, Stuart A M 2004 *Phys. Rev. E* **70** 036120
- [29] Mannella R and McClintock P V E 2012 *Fluct. Noise Lett.* **11** 1240010
- [30] Rosenbluth M N, MacDonald W M and Judd D L 1957 *Phys. Rev.* **107** 1
- [31] Öttinger H C 1966 *Stochastic Processes in Polymeric Fluids: Tools and Examples for Developing Simulation Algorithms* (Berlin: Springer) p. 112
- [32] Cohen R S, Spitzer J L and Routly P M 1950 *Phys. Rev.* **80** 230
- [33] Xiao J, Liu J, Qin H, Yu Z and Xiang N 2015 *Phys. Plasmas* **22** 092305
- [34] Ben-Israel A 1966 *J. Math. Anal. Appl.* **15** 243
- [35] Ortega J M and Rheinboldt W C 1970 *SIAM: Iterative Solution of Non-linear Equations in Several Variables* pp. 30, 181
- [36] Björck Å 1996 *SIAM: Numerical Methods for Least Squares Problems* p. 342
- [37] Broyden C G 1965 *Math. Comput.* **19** 577
- [38] He Y, Qin H, Sun Y J, Xiao J Y, Zhang R L and Liu J 2015 *Phys. Plasmas* **22** 124503
- [39] The Programming Language Lua <http://www.lua.org>
- [40] The HDF5 Library & File Format - The HDF Group <https://www.hdfgroup.org/solutions/hdf5/>
- [41] Goebel D M and Katz I 2008 *Fundamentals of Electric Propulsion: Ion and Hall Thrusters* (New York: John Wiley & Sons) chap. 1 p. 479
- [42] Huba J D 2007 *NRL Plasma Formulary* (Defense Technical Information Center) p 37
- [43] Burrage P M 1999 *Runge–Kutta Methods for Stochastic Differential Equation* (Australia: The University of Queensland Brisbane Queensland) p. 67
- [44] Burrage K and Burrage P 1999 *Physica D* **133** 34
- [45] Squire J and Qin H and Tang W M 2012 *Phys. Plasmas* **19** 084501
- [46] Kraus M 2013 *arXiv:1307.5665*
- [47] Xiao J Y, Liu J, Qin H and Yu Z 2013 *Phys. Plasmas* **20** 102517
- [48] Xiao J Y, Qin H, Liu J, He Y, Zhang R L and Sun Y J 2015 *Phys. Plasmas* **22** 112504
- [49] Kraus M, Kormann K, Morrison P J and Sonnendrücker E 2017 *J. Plasma Phys.* **83** 905830401
- [50] Klimontovich Y L 1990 *Physica A* **163** 515
- [51] Klimontovich Y L 1992 *Physica A* **182** 121
- [52] Ao P 2008 *Dyn. Commun. Theor. Phys.* **49** 1073
- [53] Hütter M and Öttinger H C 1998 *Faraday Trans.* **94** 1403